

Calcium carbonates: Induced biomineralization with controlled macromorphology

Aileen Meier¹, Anne Kastner¹, Dennis Harries², Maria Wierzbicka-Wieczorek³, Juraj Majzlan³, Georg Büchel⁴, Erika Kothe¹

¹Institute of Microbiology, Friedrich Schiller University Jena, Neugasse 25, 07743 Jena, Germany

²Institute of Geosciences, Friedrich Schiller University Jena, Analytical Mineralogy, Carl-Zeiss-Promenade 10, 07745 Jena, Germany

³Institute of Geosciences, Friedrich Schiller University Jena, General & Applied Mineralogy, Carl-Zeiss-Promenade 10, 07745 Jena, Germany

⁴Institute of Geosciences, Friedrich Schiller University Jena, Applied Geology, Burgweg 11, 07749 Jena, Germany

Correspondence to: Prof. Dr. Erika Kothe (erika.kothe@uni-jena.de)

Abstract. Biomineralization of (magnesium) calcite and vaterite by bacterial isolates has been known for quite some time.

However, the extracellular precipitation hardly has been linked to different morphologies of the minerals that are observed.

Here, isolates from limestone associated groundwater, rock and soil were shown to form calcite, magnesium calcite or

vaterite. More than 92 % of isolates indeed could form carbonates, while abiotic controls failed to form minerals. The crystal

morphologies varied, including rhombohedra, prisms and pyramid-like macro-morphologies. Using different conditions like

varying temperature, pH or media components, but also co-cultivation to test for collaborative effects of sympatric bacteria,

were used to differentiate mechanisms of calcium carbonate formation. Single crystallites were cemented with bacterial

cells; these may have served as nucleation sites by providing a basic pH at short distance from the cells. A calculation of

potential calcite formation of up to 2 g per liter of solution could link the microbial activity to geological processes.

1 Introduction

The processes of carbonate biomineralization by bacteria are usually linked to an alkaline microenvironment enhancing the

potential for carbonate precipitation at small spatial scales (Hammes and Verstraete, 2002). By microbial production of CO₂,

precipitation of calcium carbonates is favored, especially in presence of Ca²⁺. Thus, the process clearly may be defined as

microbially induced biomineralization, in contrast to microbially controlled processes best seen with intracellular,

compartment-bound formation of magnetite by magnetotactic bacteria (Yan et al., 2012 and citations therein). The cell

surface can act as a nucleation site for mineralization in induced biomineralization (Schultze-Lam et al., 1996). Since

properties are different for Gram positives and Gram negatives, both binding divalent cations such as Mg²⁺ or Ca²⁺, a

determination of the microbial clades is necessary (Chahal et al., 2011; Douglas and Beveridge, 1998; Zhu et al., 2017).

Depending on different cell surface structures, different crystal morphologies have been reported (Cao et al., 2016; Seifan et

al., 2016). Nevertheless, even from one and the same bacterial isolate, different macro-morphologies of biominerals were

Gelöscht: ;

Gelöscht: was also present

Gelöscht: in

Gelöscht: formation

Gelöscht: oti

Gelöscht: uptake

described (Tisato et al., 2015). Thus, a more thorough investigation of microbially induced biomineralization seems warranted.

The occurrence of carbonate forming bacteria has been investigated with respect to different environments (Andrei et al., 2017; Gray and Engels, 2013; Horath and Bachofen, 2009; Kang and Roh, 2016; Rusznyak et al., 2012). The process
5 generally was linked to changes induced in the direct microenvironment of the growing bacteria through metabolic features, or to providing nucleation sites for crystallization in a supersaturated environment (Roberts et al., 2013; Seifan et al., 2017; Yan et al., 2017). Either microbiomes of a specific habitat, or physiological and biomineralization properties of a single isolate have been investigated. To bridge that gap, an investigation of more isolates from one environment seems indicated.

As a result of growing knowledge on carbonate biomineralization, applications in concrete repair and formulation of self-
10 healing cement have been derived (Achal et al., 2009; Li et al., 2017; Seifan et al., 2016; Singh et al., 2015). Additionally, carbonate formation for remediation purposes has gained interest (Kumari et al., 2016; Zhu et al. 2016), including wastewater treatment (Gonzalez-Martinez et al., 2017). Basic scientific questions addressed include the nature and rates of biotic *versus* abiotic nature of calcite formation. For one species, 33 g/L calcite precipitation was reported (Seifan et al., 2016). The same assumption has been tested for the formation of rhodoliths in marine systems, where carbonate rocks evolve
15 (Cavalcanti et al., 2014). The formation of CO₂ through respiration clearly is a factor that would imply aerobic microbes (Keiner et al., 2013). Hence, a marine sediment derived limestone habitat and isolation of aerobic bacteria from that environment seemed indicated (compare Meier et al., 2017).

We thus were interested to identify different bacteria from a carbonate rock-water-soil system to address the question of how bacteria may contribute to different morphologies, even at a distance to the cells, and how much calcium carbonates may be
20 formed *in vitro* under conditions more likely to occur in nature than previously used (Castanier et al., 1999). To obtain a variety of calcium carbonate forming bacterial isolates, we focused on marine Triassic limestones exposed in central Germany. We obtained Gram-positive and Gram-negative bacteria from the limestones, and rendzina soil developed on the limestones near the limestone quarry Bad Kösen (Thuringia, Germany) and corresponding groundwater from wells probing these lithographies located nearby. The isolated bacteria represented major taxa present in the microbiomes, which were also investigated for taxonomic and physiological characterization (Meier et al., 2017). They were incubated in single culture or
25 in co-cultivation under different conditions to address biomineralization relevant to carbonate formation. With our results, we can advance the background on microbially induced biomineralization with respect to different mechanisms.

2 Material and Methods

2.1 Sampling

30 The Muschelkalk quarry in Bad Kösen is characterized by Lower Muschelkalk (Jena Formation, Lower Wellenkalk core sampled) and Middle Muschelkalk (Karstadt Formation, upper Schaumkalkbank sampled). The situation at the quarry allowed for direct access to the lithotypes by horizontally removing approximately 50 cm of stone and then coring to a depth

Gelöscht: ¶

Gelöscht: groundwater

of 20 to 30 cm from there manually to provide conditions not prone to contaminate the samples with cooling water, that would be needed for drilling devices. The rock samples were taken into fresh and sterile plastic bags and brought to the laboratory, where surface sterilization by incubation in 70 % ethanol for 30 min was performed. Afterwards, the outer part was removed with a hammer and a sterile chisel in a clean space working bench (Heraeus, Hanau, Germany), under sterile conditions.

Gelöscht: R

Gelöscht: from cores

The groundwater wells installed for monitoring purposes near Bad Kösen, in Stöben (Hy Camburg 13/198; 4478864N, 5660183E; Lower Muschelkalk sampled at 34 m depth) and Wichmar (Hy Camburg 121/1988; 4478030N, 5655906E; 120 m, Middle Muschelkalk sampled at 17 m) were sampled with the help of an electric pump MPI (Grundfos, Bjerringbro, Denmark) after reaching constant pH and temperature. All samples were stored at 6 °C prior to analysis.

Soil was sampled at 40 cm depth from 15 sampling points at the Bad Kösen quarry for rendzina on the respective limestone bed in a radius of about 1 km and homogenized.

2.2 Isolation and characterization of bacteria

For the isolation of bacteria from the limestones, Std I (Carl Roth, Roth, Germany; supplied with NaCl at 3, 5, 7 % if indicated by sample chemistry), minimal AM (Amoroso et al., 2002) and oligotrophic R₂A (Reasoner and Geldreich, 1985) media were applied. Calcification promoting B-4 medium without pH adjustment (Banks et al., 2010) was used for isolating limestone associated bacteria.

For rock samples, 5 g of powdered rock sample were added to 45 ml sterile 0.9 % NaCl, followed by vortexing for 20 min.

Subsequently, sonication was applied for 15 min and filtered (Sartorius, Göttingen, Germany) supernatant was plated. In addition, a dilutions in 0.9 % NaCl was prepared without filtering and cultured in liquid medium, or particles were directly placed on nutrient agar to account for different amounts of bacteria in samples.

[1] verschoben

Gelöscht: as small particles

A total of 2.5 L of groundwater samples were filtered before culturing using 0.2 µm membrane filters (Omnipore membrane filters, Millipore) in a filtration system (GP Millipore Express plus membrane, Merck Millipore, Darmstadt, Germany). The filters were placed on agar and incubated at 10 °C for three days. Additionally, after washing off the filters a dilution series in sterile 0.9 % NaCl solution was plated.

Gelöscht: ere

Gelöscht: Surface sterilized rock samples were powdered and dilution series were prepared.

[1] nach oben: cultured in liquid medium or placed as small particles on nutrient agar.

Gelöscht: ¶

Gelöscht: before adding to cultures

Gelöscht: and

Independent from the origin of samples, pure cultures were obtained by serial plating. Soil extracts from 100 g mixed soil samples, dried at 40 °C overnight were prepared using 500 ml 10 mM 3-(N-morpholino)propanesulfonic acid (MOPS, Serva, Heidelberg, Germany). The suspension was incubated at 28 °C for 1 hour prior to filtration with a vacuum pump system. The soil extract was supplemented with 100 mg/L glucose, 1 mg/L casein hydrolysate, 1 mg/L yeast extract and 18 mg/L agar and sterilized. This soil extract medium was then used for cultivation of isolates obtained from rock or soil samples.

Incubation was performed at 28 °C and 10 °C for 3 to 5 days in duplicates, with constant shaking at 120 rpm for liquid cultures under dark conditions.

For strain identification, genomic DNA (DNeasy Power Soil kit, Qiagen, Hildesheim, Germany) was extracted from pure cultures and 16S rDNA was amplified (primers 27F and 1492r at 100 mM, 0.02 U Dream Taq polymerase, 1 x Dream Taq

buffer, 100 mM deoxynucleotide triphosphate mixture, 1 µl DNA template; [Thermo Fisher, Schwerte, Germany](#)) with 30 cycles (95 °C for 3 min, followed by cycles of 95 °C for 30 sec, 57-60 °C for 30-45 sec, 72 °C for 60-90 sec, with final step at 72 °C for 10-30 min) and [bidirectionally](#) sequenced [using Sanger biochemistry](#) ([GATC Biotech, Konstanz, Germany](#)). The obtained sequences were assembled *via* Bioedit sequence alignment editor version 7.1.3.0 (<http://www.mbio.ncsu.edu/BioEdit/bioedit.html>) and analyzed using NCBI BLAST tool (<http://www.ncbi.nlm.nih.gov>, see also supplemental Tab. S1). All obtained sequences were made available with NCBI GenBank ([accession numbers KX527662-KX527725, KX536502- KX536520, KX570902- KX570911, KX573089- KX573101](#); see [suppl. Tab. S1](#); see Meier et al., 2017). The strains are deposited with the Jena Microbial Resource Collection ([Jena, Germany](#)).

Gelöscht: c

Gelöscht: s

2.3 Biomineralization assays

To study effects on carbonate mineralization, B-4 agar plates or liquid cultures were incubated at 28 °C or 10 °C for one to three weeks. CaCO₃ (B-4CO) or Ca₃(PO₄)₂ (B-4CP) as source of calcium were used replacing the calcium acetate of the medium [to evaluate different calcium mobilization activities of the strains applied](#). For differentiation between biological and chemical mechanisms, non-inoculated plates and plates streaked with dead biomass were used as negative controls. Bromthymol blue (0.3 %; Merck, Darmstadt) was used [for plates assessing pH shifts](#). [Using the strains of one habitat \(suppl. Tab. S1\), co-inoculation plates were produced to test for competition or induction of biomineralization by streaking out the strains crossing each other on B-4 agar. Two- or four-strain interactions were tested using sympatric isolates from the same habitat.](#)

Gelöscht: as

Gelöscht: indicator where appropriate

Gelöscht: Selected experiments were designed to investigate

Gelöscht: activities of the bacterial strains

Gelöscht: ed towards

Gelöscht: com

Gelöscht: ot

2.4 Mineralogical investigations

Solid products were visualized with a stereomicroscope (Zeiss, [Jena, Germany](#)) and sampled [under the binocular using sterile tweezers with as little as possible bacteria attached into](#) 0.2 ml reaction tubes. Powder X-ray diffractometer (Bruker D8 Advance; [Bruker, Ettlingen, Germany](#)) with Cu K α radiation ($\lambda=1.54058 \text{ \AA}$) and LynxEye detector ([Bruker, Ettlingen, Germany](#)) was used on powdered crystals transferred to a zero-background silicon sample holder and measured with following parameters: 18-70 °2 θ , a step size of 0.02 °2 θ and dwell of 0.5 sec.

Scanning electron micrographs (SEM; Quanta 3D FEG; FEI) were taken from [samples placed on a sample holder and sputtered with carbon or gold without additional preparation and then](#) imaged in secondary (SE) or back-scattered electron mode (BSE) at an acceleration voltage of typically 10 kV. Semi-quantitative chemical analysis was conducted using an energy-dispersive X-ray (EDX) spectrometer (EDAX, Mahwah).

Gelöscht: sputtered samples

2.5 Quantification of precipitate formation

Liquid medium inoculated with *Agrococcus jejuensis* SMM51, *Bacillus muralis* rLMd or *Bacillus* sp. rMM9 was incubated at 28 °C [and 150 rpm shaking in the dark](#) for at least three weeks. Precipitates were harvested using a sterile cell strainer (easystrainer, 40µm for 50 ml tubes, [Greiner, Frickenhausen, Germany](#)) and rinsed with pure water to separate cells from the

Formatiert: Schriftart: Nicht Kursiv

Gelöscht: BO

solids. The crystals were dried and weighed. Bacterial growth was determined with cells diluted 1:1000 with ISOTON Diluent (Beckman Coulter, Brea, CA, USA) in a Coulter cell counter (Beckman Coulter, Brea, CA, USA) in triplicates.

For calculation of yearly biomineral formation, we used the amount produced in our cultures (approx. 100 mg) during the time of incubation (3 weeks) to calculate how much this would make in 52 weeks, a full year. 1700 mg would be the result of such an approximate calculation for new mineral formation during a year. This is an underestimation, since the nucleation time is needed only once.

3. Results

3.1 Biomineralization activities of bacterial isolates

This study is focused on 138 bacterial isolates belonging to Proteobacteria (7 Alpha-, 7 Beta-, 35 Gammaproteobacteria), Bacteroidetes (5 isolates), Actinobacteria (47 strains) and Firmicutes (37 isolates; Tab. S2) from two different limestones, Lower Muschelkalk (LM) and Middle Muschelkalk (MM), and three compartments for each lithotype representing rock (r), groundwater (gw) and soil (s). We used the total of 138 isolates to test, whether they are able to form biominerals under laboratory conditions. Only 10 of these isolates (7.2 %) formed no crystals when tested on five solid and one liquid medium and at two temperatures. There were no obvious differences between isolates obtained from the six habitats (Fig. 1 through Fig. 6). This shows that in a carboniferous environment, strains forming carbonates are highly enriched.

As to the means of inducing mineralization, the influence of pH could be tested. While 89 strains did not change medium pH, 43 produced an alkaline environment supportive of carbonate formation (Fig. 1 through Fig. 6). However, two of those alkalinity producing strains did not produce biominerals (rMM21, see Fig. 2, and W_5.3a, see Fig. 4), all other non-producers did not change pH. In addition, crystal formation was observed with all strains which actually lowered pH (Fig. 1 through Fig. 6). The temperature clearly had an effect, although there was no clear correlation. While on one medium, higher temperature might have induced formation of crystals not observed at low temperature, the opposite effect was visible on the next medium (compare, e.g., rLM4.3, Fig. 1). Any combination of traits was observed. This indicates that rather differences among strains than a mere general influence on the micro-environmental conditions leading to abiotic carbonate formation was observed.

The highest incidence of mineral production was observed with soil isolates obtained from soil developed on Middle Muschelkalk (Fig. 6). Biomineralization potential was not associated to phylogeny. To give an example, eight isolates of the genus *Bacillus* (compare suppl. Tab. S2) isolated from Lower Muschelkalk rock samples induced precipitation (Fig. 1), whereas six strains of the same genus (S_H4, S_Sd8, S_Sd9, S_29, see Fig. 3, and W_B4 and W_Sd8, Fig. 4) were negative in biomineralization.

Gelöscht: Of

Gelöscht: 40

Gelöscht: o

Gelöscht: under the conditions tested

Gelöscht: Figs. 1-6

Gelöscht: E

3.2 Identification of calcium carbonate biominerals

From each habitat, the four most prevalent isolates as judged by colony morphology during isolation were selected for further study (Tab. 1). Of these 24 strains, 17 were Gram positives, representing the taxa *Agrococcus*, *Agromyces*, *Arthrobacter*, *Micrococcus*, *Rhodococcus* and *Streptomyces* (all Actinobacteria), and *Bacillus*, *Planococcus*, *Psychrobacillus*, *(Firmicutes)*. The seven Gram negative genera were *Flavobacterium* (Bacteroidetes), *Ochrobactrum*, *Sphingopyxis* (Alphaproteobacteria), *Advenella* (Betaproteobacteria), *Lelliottia*, *Moraxella*, and *Pseudomonas*, (Gammaproteobacteria). Again, there was no correlation between medium or temperature preference and biomineralization visible (compare Fig. 1 through Fig. 6 and suppl. Tab. S2).

Powder X-ray diffraction and EDX analyses identified mostly calcite, less frequently vaterite and magnesium calcite (see Tab. 1). Calcite formed on cultures from rock of Lower Muschelkalk *Bacillus* sp. rLMa, *Micrococcus luteus* rLMc and *B. muralis* rLMd and Middle Muschelkalk *Agrobacter pascens* rMM19 and *Ochrobactrum intermedium* rMM23. Of these, *B. muralis* rLMd and *Agrobacter pascens* rMM19 formed calcite as well as vaterite. No magnesium calcite was found with strains isolated from rock samples. The groundwater isolates showed lowest incidence but high variability of biomineralization with *Arthrobacter* sp. W_2.1 forming vaterite, while *Advenella* sp. W_Sd3 and *Rhodococcus erythropolis* W_Sd5 were found to form vaterite and magnesium calcite. All three phases were present in one example, a strain obtained from soil of Lower Muschelkalk, *Streptomyces* sp. SLM5. Soil isolates from Middle Muschelkalk *Streptomyces* sp. sMM10 and *Sphingopyxis bauzanensis* sMM41 formed vaterite and magnesium calcite, while *Agrococcus jejuensis* sMM crystallized calcite and vaterite.

3.3 Variation in crystal morphologies

Color and morphology of crystal aggregates were highly variable, ranging from colorless to brownish or purple, and morphologies from individual rhombohedral crystals, round or acicular aggregates or rosettes to laminated crusts. Aggregates located within the agar mostly formed small rhombohedra or spheres.

Biominerals were on top or below the biomass; for some strains the crystals formed always in a certain distance from the colonies, which might indicate a zone of change in pH around the culture (Fig. 7). Indicator plates with bromthymol blue indicated mainly change to basic pH > 7.6, followed by crystal precipitation. A few isolates of each environment revealed acidification, most pronounced for Lower Muschelkalk *Bacillus* strains and Middle Muschelkalk *Streptomyces* with pH < 6.0.

A recurring morphological feature was subparallel intergrowth of μm to sub- μm sized crystallites. In simple cases, the resulting aggregates resembled the morphology of a single crystal, in other cases, more complex aggregates were found (Fig. 8; for further morphologies of other isolates, see supplemental Fig. S1). Crystal aggregates produced by *L. amnigena* S_H3 exhibited platy crystals arranged into a rosette.

Gelöscht: *Bacillus*, *Micrococcus*, *Planococcus*, *Psychrobacillus*, *Rhodococcus* and *Streptomyces*

Gelöscht: *Advenella*, *Agromyces*,

Formatiert: Schriftart: Nicht Kursiv

Formatiert: Schriftart: Nicht Kursiv

Formatiert: Schriftart: Nicht Kursiv

Gelöscht: *Moraxella*, *Ochrobactrum*, *Pseudomonas*, and *Sphingopyxis*

Formatiert: Schriftart: Nicht Kursiv

Formatiert: Schriftart: Nicht Kursiv

Gelöscht: T

Formatiert: Schriftart: Nicht Kursiv

Gelöscht: concomitantly

Formatiert: Schriftart: Nicht Kursiv

Formatiert: Schriftart: Nicht Kursiv

Formatiert: Schriftart: Nicht Kursiv

Formatiert: Schriftart: Nicht Kursiv

3.4 Impact of cultivation conditions

Phenotypic differences in crystal morphology were readily observed, dependent also on temperature (Fig. 8). To show two examples, *Pseudomonas* sp. S_1.1 formed laminated shapes at 28 °C (A) and transparent spheres at 10 °C. At the lower temperature, pigment formation was induced to a large extent. *Rahnella* sp. S_H1 induced rhombohedral to rosette like crystals at higher temperature. At 10 °C, small white spheres were produced.

On plates containing calcium carbonate or calcium phosphate, more bacterial growth, but less biomineralization was observed. On the medium with CaCO₃, the groundwater isolates showed temperature-dependent biomineralization. Crystals were formed at 10 °C, whereas the temperature of 28 °C induced mineral dissolution indicated by halo formation.

3.5 Direct impact of bacteria

The bacterial influence was visible also by direct associations. *R. erythropolis* Wsd5 crystals were coated by bacterial cells (Fig. 9). Some areas free of cells contained oval, clearly delimited holes of the same size and shape as the surrounding bacterial cells. Occasionally, these holes were characterized by an extended trace (a tail) on one side. *Lelliottia amnigena* S_H3 formed rosettes which show a laminated structure upon higher magnification, again with holes in the leaflets.

Two or four strains of one community were co-cultivated to determine their interactions. There was either no interaction, inhibition leading to lack of growth, or parasitism visible by overgrowing the competing strain(s). Concerning biomineralization, the co-cultivation had either no effect, or it enhanced precipitation, producing larger crystals in the contact zone (Tab. 2). The biotic interactions showed an impact on biomineralization, e.g. with more crystals being produced in the interaction zone between *L. amnigena* S_H3 and *Pseudomonas* sp., or reduced formation of crystals at the contact zone between *Micrococcus luteus* rLMc and *Bacillus muralis* rLMd (suppl. Fig. S2). In addition, the strains showed different responses towards each other. *Advenella* sp. W_Sd3 from groundwater of Middle Muschelkalk was overgrown by all interaction partners without a change in crystal distribution, and *Streptomyces* sp. sLM17 from the Middle Muschelkalk rock sample inhibited *A. cerinus* sLM10 without crystal formation.

3.6 Quantification of precipitates

The quantification of crystals formed resulted in similar cell counts ranging from $2.06 \cdot 10^7$ to $8.65 \cdot 10^7$. Since the bacterial biomass within the centrifugation pellet thus was similar, the dry mass was compared to see different rates of biomineral formation. The dry weight of precipitates varied, with highest amounts and thus the highest ability for crystal formation seen with *Bacillus* sp. rMM9 (0.104 g/L), followed by *Agrococcus jejuensis* sMM 51 (0.096 g/L). *Bacillus muralis* rLMd demonstrated the lowest amount of crystals with 0.064 g/L (Tab. 3).

Gelöscht: 9

Gelöscht: see

Gelöscht: 8

Gelöscht: with more crystals developing at the contact zones

Formatiert: Schriftart: Kursiv

Formatiert: Schriftart: Kursiv

Formatiert: Schriftart: Kursiv

Formatiert: Schriftart: Nicht Kursiv

Formatiert: Schriftart: Nicht Kursiv

Formatiert: Schriftart: Nicht Kursiv

4. Discussion

Microbially induced calcite precipitation has been known as a general phenomenon since the 1970's and found application in different fields such as cementation of cracks in historical memorials, buildings or sculptures made of limestone by cementing cracks, mostly through ureolytic bacteria (van Tittelboom et al., 2010; Wong, 2015; Zhu and Dittrich, 2016). The general availability of bacterial isolates from different environments associated with limestones, however, was not accessed to the full (Gonzales-Martinez et al., 2017; Seifan et al., 2017). Here, two lithotypes of Lower and Middle Muschelkalk were assessed for the prevalence of carbonate precipitating bacteria.

Calcite, magnesium calcite and vaterite could be formed by the bacteria growing on standard laboratory media. Since vaterite occurs in aqueous, supersaturated solutions, high water content in the precipitates might be explained with water available from the agar. Magnesium calcite was likely formed when the bacterial cell surfaces accumulated the element (see also Cui et al., 2015; Rusznyak et al., 2012). Few trace elements, such as sulfur, chloride and phosphorus probably originating from cell components or salts included in the medium have been detected (see also Rivadeneyra et al., 2000).

Different crystal aggregates with macro-morphologies such as rhombohedra, rosettes and spheres were detected, occurring either in the medium at a distance to the inoculated bacteria, or below or on top of the cultures. Morphological variations of crystal shapes revealed a microbial impact on mineral precipitation (compare Branson et al., 2016). Crystal colors by impurities incorporated in the lattice such as salts or secreted pigments were clearly observed, as calcite can incorporate metal ions in its crystal structure (Kang et al., 2014).

With respect to alkaline pH favorable for calcium carbonate precipitation, a probable process might be the ammonification of amino acids, deriving from yeast extract added to the medium. By degrading amino acids, ammonia develops which increases the pH to alkaline conditions. So far, mostly urease activity has been implied for pH increase in biogenic calcite formation (Bachmeier et al., 2002; Okyay et al. 2016; Wei-Soon et al., 2012). However, our results with strains acidifying the medium and still precipitating calcium carbonate clearly shows that other mechanisms are involved as well.

Biotic effects were investigated by co-cultivation. Several inter-species reactions might influence the outcome of biomienral production. For an easy way to interpret interactions, growth should be considered. E.g., growth inhibition of a sympatric strain could be a result of secreted antimicrobial compounds or competition (Hibbing et al., 2009). Growth promotion, like with *Flavobacterium limicola* S_5.3, also may be due to growth promoting compounds for interspecies communication of xenosiderophore use. Another explanation would be the change of the medium to alkaline pH that might well improve the growth of crystals that are nucleated by virtue of the second strain. Or the interaction leads to activation of genes involved in mineral formation. Thus, interactions between two to four strains were tested. For this experiment, strains were chosen that came from the same environment to improve the probability of interactions in nature. Increased crystallization at contact zones was noticed in specific bacterial combinations, e.g. with *Rhizobium* sp. S_4.1a and *Pseudomonas* sp. S_H4.

Biogenic calcite precipitation may contribute to limestone sedimentation (compare Garcia et al., 2016). With 0.104 g/L dry weight for *Bacillus* sp. rMM9, a high yield of carbonate precipitation was found. Bacterial cells, especially spores with their

Gelöscht: G

Gelöscht: compatriote

Gelöscht:

Formatiert: Schriftart: Nicht Kursiv

Formatiert: Schriftart: Nicht Kursiv

Formatiert: Schriftart: Nicht Kursiv

high surface to volume ratio and specific cell wall structure, can serve as nucleation sites. Spores encapsulated by calcite might survive for long periods of time, and can be reactivated, followed by germination and growth of new bacterial generations (Murai and Yoshida, 2013). Hence, ample sporulation may explain differences in the amounts recorded between different strains of the genus *Bacillus* (Yasuda-Yasaki et al., 1978).

5 Bacteria are known to contribute to the growth of carbonate stalactites that grow by a few mm per year (Genty et al., 2011). Comparing these observations to our experiment, bacterial isolates may exert a meaningful impact on limestone deposition.

In our experiment, 104 mg/L had been formed after three weeks. From this, up to 2 g/L can be calculated to be formed over the course of one year. This compares well to a model experiment which resulted in ~ 2 g abiotic CaCO₃/yr (Short et al., 2005). As we could show increase in productivity in mutual interactions, microbial communities might well reach even

Gelöscht: From the

Gelöscht: yearly

10 higher rates (Castanier et al., 1999).

As a main result of our investigation of 138 isolates of two lithotypes of limestone in Germany, we can conclude that (magnesium) calcite and vaterite production can be induced through medium alkalinity, through direct surface interaction for nucleation visible in close associations, but also in acidified media and a distance apart from the growing bacteria. This indicates, that within the microbially induced calcium carbonate precipitation, mechanistically different routes of

Gelöscht: 140

15 biomineralization are possible. The control of morphologies at a distance to the colony seems specifically interesting. We propose that molecules secreted by the bacteria, e.g. specific proteins, might lead to preferential crystal growth at different mineral surfaces due to coating. This clearly warrants further, more molecular studies.

Acknowledgements

The authors would like to thank Falko Langenhorst, Dirk Merten, Thomas Wach, Hans-Martin Dahse and Justus Linden for help with measurements. The International Max-Planck Research School "Global Biogeochemical Cycles" and the Jena School for Microbial Communication (GSC124) are thanked for financial support. EK wishes to acknowledge DFG-CRC 20 1127.

References

- Achal, V., Mukherjee, A., Basu, P.C., and Reddy, M.S.: Strain improvement of *Sporosarcina pasteurii* for enhanced urease and calcite production, *J. Ind. Microbiol. Biotechnol.*, 36, 981-988, 2009.
- 25 Amoroso, M.J., Schubert, D., Mitscherlich, P., Schumann, P., and Kothe, E.: Evidence for high affinity nickel transporter genes in heavy metal resistant *Streptomyces spec.*, *J. Basic Microbiol.*, 40, 295-301, 2000.
- Andrei, A.S., Pausan, M.R., Tamas, T., Har, N., Barbu-Tudoran, L., Leopold, N., and Manciu, H.L.: Diversity and biomineralization potential of the epilithic bacterial communities inhabiting the oldest public stone monument of Cluj-
- 30 Napoca (Transylvania, Romania), *Front. Microbiol.*, 8, 372, 2017.

- Bachmeier, K.L., Williams, A.E., Bang, S.S., and Warmington, J.R.: Urease activity in microbiologically-induced calcite precipitation, *J. Biotechnol.* 93, 171–181, 2002.
- Banks, E.D., Taylor, N.M., Gulley, J., Lubbers, B.R., Giarrizzo, J.G., Bullen, H.A., Hoehler, T.M., and Barton, H.A.: Bacterial calcium carbonate precipitation in cave environments: A function of calcium homeostasis, *Geomicrobiol. J.* 27, 444-454. 2010.
- 5 Branson, O., Bonnin, E.A., Perea, D.E., Spero, H.J., Zhu, Z., Winters, M., Hönisch, B., Russell, A.D., Fehrenbacher, J.S., and Gagnon, A.C.: Nanometer-scale chemistry of a calcite biomineralization template: Implications for skeletal composition and nucleation, *Proc. Natl. Acad. Sci. U.S.A.* 113, 12934-12939, 2016.
- Castanier, S., Le Métayer-Levreil, G., and Perthuisot, J.-P.: Ca-carbonates precipitation and limestone genesis - the microbiogeologist point of view, *Sediment. Geol.* 126, 9-23. 1999.
- 10 Chahal, N., Rajor, A., and Siddique, R.: Calcium carbonate precipitation by different bacterial strains, *Afric. J. Biotechnol.* 10, 8359-8372, 2011.
- Cao, C., Jiang, J., Sun, H., Huang, Y., Tao, F., and Lian, B.: Carbonate mineral formation under the influence of limestone-colonizing actinobacteria: Morphology and polymorphism, *Front. Microbiol.* 7, 366, 2016.
- 15 Cavalcanti, G.S., Gregoracci, G.B., dos Santos, E.O., Silveira, C.B., Meirelles, P.M., Longo, L., Gotoh, K., Nakamura, S., Iida, T., Sawabe, T., Rezende, C.E., Francini-Filho, R.B., Moura, R.L., Amado-Filho, G.M., and Thompson, F.L.: Physiologic and metagenomic attributes of the rhodoliths forming the largest CaCO₃ bed in the South Atlantic Ocean, *ISME J.* 8, 52-62. 2014.
- Cui, J., Kennedy, J.F., Nie, J., and Ma, G.: Co-effects of amines molecules and chitosan films on in vitro calcium carbonate mineralization, *Carbohydr. Polym.* 133, 67-73, 2015.
- 20 Douglas, S., and Beveridge, T.J.: Mineral formation by bacteria in natural microbial communities, *FEMS Microbiol. Ecol.* 26, 79-88, 1998.
- García, G.M., Márquez, G.M.A., and Moreno, H.C.X.: Characterization of bacterial diversity associated with calcareous deposits and drip-waters, and isolation of calcifying bacteria from two Colombian mines, *Microbiol. Res.* 182, 21-30, 2016.
- 25 Genty, D., Baker, A., and Vokal, B.: Intra- and inter-annual growth rate of modern stalagmites, *Chem. Geol.* 176, 191–212, 2011.
- Gonzalez-Martinez, A., Rodriguez-Sanchez, A., Rivadeneyra, M.A., Rivadeneyra, A., Martín-Ramos, D., Vahala, R., and Gonzalez-Lopez, J.: 16S rRNA gene-based characterization of bacteria potentially associated with phosphate and carbonate precipitation from a granular autotrophic nitrogen removal bioreactor, *Appl. Microbiol. Biotechnol.* 101, 817-829. 2017.
- 30 Gray, C.J., and Engel, A.S.: Microbial diversity and impact on carbonate geochemistry across a changing geochemical gradient in a karst aquifer, *ISME J.* 7, 325-337, 2013.

- Hammes, F., and Verstraete, W.: Key roles of pH and calcium metabolism in microbial carbonate precipitation, *Environ. Sci. Biotechnol.* 1, 3-7, 2002.
- Hibbing, M.E., Fuqua, C., Parsek, M.R., and Peterson, S.B.: Bacterial competition: surviving and thriving in the microbial jungle, *Nature Rev. Microbiol.* 8, 15-25, 2009.
- 5 Horath, T., and Bachofen, R.: Molecular characterization of an endolithic microbial community in dolomite rock in the central Alps (Switzerland), *Microbial Ecol.* 58, 290-306, 2009.
- Kang, S.K., and Roh, Y.: Microbially-mediated precipitation of calcium carbonate nanoparticles, *J. Nansci. Nanotechnol.* 16, 1975-1978, 2016.
- Kang, C.-H., Han, S.-H., Shin, Y., Oh, S.J., and So, J.-S.: Bioremediation of Cd by microbially induced calcite precipitation, *Appl. Biochem. Biotechnol.* 172, 2907-2915, 2014.
- 10 Keiner, R., Frisch, T., Hanf, S., Rusznyak, A., Akob, D.M., Küsel, K., and Popp, J.: Raman spectroscopy - an innovative and versatile tool to follow the respirational activity and carbonate biomineralization of important cave bacteria, *Anal. Chem.* 85, 8708-8714, 2013.
- Kumari, D., Qian, X.Y., Pan, X., Achal, V., Li, Q., and Gadd, G.M.: Microbially-induced carbonate precipitation for immobilization of toxic metals, *Adv. Appl. Microbiol.* 94, 79-108, 2016.
- 15 Li, M., Zhu, X., Mukherjee, A., Huang, M., and Achal V.: Biomineralization in metakaolin modified cement mortar to improve its strength with lowered cement content, *J. Hazard. Mater.* 329, 178-184, 2017.
- Meier, A., Singh, M.K., Kastner, A., Merten, D., Büchel, G., and Kothe, E.: Microbial communities in carbonate rocks - from soil via groundwater to rocks, *J. Basic Microbiol.*, in press.
- 20 Murai, R., and Yoshida, N.: *Geobacillus thermoglucosidasius* endospores function as nuclei for the formation of single calcite crystals, *Appl. Environ. Microbiol.* 9, 3085-3090, 2013.
- Okyay, T.O., Nguyen, H.N., Castro, S.L., and Rodrigues, D.F.: CO₂ sequestration by ureolytic microbial consortia through microbially-induced calcite precipitation, *Sci. Total Environ.* 572, 671-680, 2016.
- Reasoner, D.J., and Geldreich, E.E.: 1985. A new medium for the enumeration and subculture of bacteria from potable water, *Appl. Environ. Microbiol.* 49, 1-7, 2016.
- 25 Rivadeneira, M.A., Delgado, G., Soriano, M., Ramos-Cormenzana, A., and Delgado, R.: Precipitation of carbonates by *Nesterenkonia halobia* in liquid media, *Chemosphere* 41, 617-624, 2000.
- Roberts, J.A., Kenward, P.A., Fowle, D.A., Goldstein, R.H., Gonzales, L.A., and Moore, D.S.: Surface chemistry allows for abiotic precipitation of dolomite at low temperature, *Proc. Natl. Acad. Sci. U.S.A.* 110, 14540-14545, 2013.
- 30 Rusznyak, A., Akob, D.M., Nietsche, S., Eusterhues, K., Totsche, K.U., Neu, T.R., Frosch, T., Popp, J., Keiner, R., Geletnek, J., Katzschmann, L., Schulze, E.D., and Küsel, K.: Calcite biomineralization by bacterial isolates from the recently discovered pristine karstic Herrenberg cave, *Appl. Environ. Microbiol.* 78, 1157-1167, 2012.
- Schultze-Lam, S., Fortin, D., Davis, B.S., and Beveridge, T.J.: Mineralization of bacterial surfaces, *Chem. Geol.* 132, 171-181, 1996.

- Seifan, M., Samani, A.K., and Berenjian, A.: Bioconcrete: next generation of self-healing concrete, *Appl. Microbiol. Biotechnol.* 100, 2591-2602, 2016.
- Seifan, M., Samani, A.K., and Berenjian, A.: New insights into the role of pH and aeration in the bacterial production of calcium carbonate (CaCO₃), *Appl. Microbiol. Biotechnol.* 101, 3131-3142, 2017.
- 5 Short, M.B., Baygents, J.C., Beck, W.J., Stone, D.A., Toomey III, R.S., and Goldstein, R.E.: Stalactite growth as a free-boundary problem: A geometric law and its platonic ideal, *Phys. Rev. Lett.* 94, 018501, 2005.
- Singh, R., Yoon, H., Sanford, R.A., Katz, L., Fouke, B.W., and Werth, C.J.: Metabolism-induced CaCO₃ biomineralization during reactive transport in a micromodel: Implications for porosity alteration, *Environ. Sci. Technol.* 49, 12094-12104, 2015.
- 10 Tisato, N., Torriani, S.F., Monteux, S., Saure, F., De Waele, J., Tacagna, M.L., D'Angeli, I.M., Chailloux, D., Renda, M., Eglinton, T.I., and Bontognali, T.R.: Microbial mediation of complex subterranean mineral structures, *Sci. Rep.* 5, 15525, 2015.
- van Tittelboom, K., De Belie, N., De Muynck, W., and Verstraete, W.: Use of bacteria to repair cracks in concrete, *Cement Concr. Res.* 40, 157-166, 2010.
- 15 Wei-Soon, N., Lee, M.-L., and Hii, S.-L.: An overview of the factors affecting microbial-induced calcite precipitation and its potential application in soil improvement, *Int. J. Civic Environ. Struct. Constr. Architect* 6, 188-194, 2012.
- Wong, L.S.: 2015. Microbial cementation of ureolytic bacteria from the genus *Bacillus*: a review of the bacterial application on cement-based materials for cleaner production, *J. Cleaner Product* 93, 5-17, 2012.
- Yan, W., Xiao, X., and Zhang, Y.: Complete genome sequence of *Lysinibacillus sphaericus* LMG 22257, a strain with ureolytic activity inducing calcium carbonate precipitation, *J. Biotechnol.* 246, 33-35, 2017.
- 20 [Yan, L., Zhang, S., Chen, P., Liu, H., Yin, H., Li, H.: Magnetotactic bacteria, magnetosomes and their application, *Microbiol. Res.* 167, 507-519, 2012.](#)
- Yasuda-Yasaki, Y., Namiki-Kanie, S., and Hachisuka, Y.: Inhibition of *Bacillus subtilis* spore germination by various hydrophobic compounds: demonstration of hydrophobic character of L-alanine receptor site, *J. Bacteriol.* 136, 484-490, 1978.
- 25 Zhu, T., and Dittrich, M.: Carbonate precipitation through microbial activities in natural environment, and their potential in biotechnology: A review, *Front. Bioengin. Biotechnol.* 4, 4, 2016.
- Zhu, X., Li, W., Zhan, L., Huang, M., Zhang, Q., and Achal, V.: The large-scale process of microbial carbonate precipitation for nickel remediation from an industrial soil, *Environ. Pollut.* 19, 149-155, 2016.
- 30 Zhu, Y., Ma, N., Jin, W., Wu, S., and Sun, C.: Genomic and transcriptomic insights into calcium carbonate biomineralization by marine actinobacterium *Brevibacterium linens* BS258, *Front. Microbiol.* 8, 602, 2017.

Table 1: Biomineral identification by Powder X-ray diffraction and EDX analyses from strains obtained from groundwater (gw), rock (r) and soil (s) samples from Lower (LM) and Middle Muschelkalk (MM) and grown on B-4 agar plates.

| Isolate Source | Strain | Calcite | Vaterite | Magnesium calcite |
|----------------|---------------------------------------|---------|----------|-------------------|
| rLM | <i>B. niacini</i> rLM1.4 | + | + | - |
| | <i>Bacillus</i> sp. rLMA | + | - | - |
| | <i>Micrococcus luteus</i> rLMc | + | - | - |
| rMM | <i>Bacillus muralis</i> rLMd | + | + | - |
| | <i>Bacillus</i> sp. rMM9 | + | + | - |
| | <i>Agrobacter pascens</i> rMM19 | + | + | - |
| gwLM | <i>Ochrobactrum intermedium</i> rMM23 | + | - | - |
| | <i>Pseudomonas</i> sp. S_1.1 | + | - | - |
| | <i>Microbacterium</i> sp. S_2.10 | + | + | - |
| gwMM | <i>B. sharmana</i> S_3.1 | - | - | + |
| | <i>Rhizobium</i> sp. S_4.1 | + | - | - |
| | <i>Rahnella</i> sp. S_HI | + | + | - |
| | <i>Arthrobacter</i> sp. W_2.1 | - | + | - |
| | <i>C. koreensis</i> W_5.3b | + | - | + |
| | <i>Flavobacterium</i> sp. W_5.4 | + | + | + |
| | Uncultured <i>Leifsonia</i> sp. W_Sd1 | - | + | + |
| sLM | <i>Advenella</i> sp. W_Sd3 | - | + | + |
| | <i>Rhodococcus erythropolis</i> W_Sd5 | - | + | + |
| | <i>Streptomyces</i> sp. sLM5 | + | + | + |
| sMM | <i>B. frigiditolerans</i> sLM13 | - | - | + |
| | <i>Paenibacillus</i> sp. sLM29 | + | - | - |
| | <i>Streptomyces</i> sp. sMM10 | - | + | + |
| | <i>P. umidemergens</i> sMM17 | + | - | - |
| | <i>S. maltophilia</i> sMM31 | + | + | - |
| sMM | <i>Sphingopyxis bauzanensis</i> sMM41 | - | + | + |
| | <i>Bacillus</i> sp. sMM46 | - | - | + |
| | <i>Agrococcus jejuensis</i> sMM51 | + | + | - |

+, detected; -, not detected

Formatiert: Schriftart: Nicht Kursiv

Table 2: Growth and biomineralization of pairwise co-cultured bacterial isolates from groundwater (gw), rock (r) and soil (s) samples from Lower (LM) and Middle Muschelkalk (MM).

| | Growth | Biom mineralization |
|--|---|--|
| rLM | | |
| <i>Micrococcus luteus</i> rLMc | Inhibited <i>B. simplex</i> 3.3F | - |
| <i>Bacillus muralis</i> rLMd | Highest growth rate, overgrew all interaction strains | - |
| <i>Bacillus</i> sp. rLMa | | - |
| <i>Bacillus simplex</i> 3.3F | Inhibited by <i>B. muralis</i> rLMd | At contact point to <i>Bacillus</i> sp. rLMa, increased |
| rMM | | |
| <i>Bacillus</i> sp. rMM8 | Highest growth rate, overgrew <i>O. intermedium</i> rMM23 | Increased crystal accumulation at contact point to <i>A. pascens</i> rMM 19 |
| <i>Agrobacter pascens</i> rMM19 | +/- | Crystals at contact point to <i>Bacillus</i> sp. rMM8 |
| <i>Psychrobacillus psychrodurans</i> rMM20 | +/- near contact point to <i>Bacillus</i> sp. rMM8 | Crystals at contact point to <i>Bacillus</i> sp. rMM8 |
| <i>Ochrobactrum intermedium</i> rMM23 | | No change in biomineralization |
| gwLM | | |
| <i>Leliottia amnigena</i> S_H3 | Highest growth rate, overgrew competitors | At contact points increased |
| <i>Pseudomonas</i> sp. S_H4 | | - |
| <i>Rhizobium</i> sp. S_4.1a | | - |
| <i>Flavobacterium limicola</i> S_5.3 | | - |
| gwMM | | |
| <i>Advenella</i> sp. W_Sd3 | Overgrown by all interaction partners | - |
| <i>Rhodococcus erythropolis</i> W_Sd5 | Inhibited by <i>Planococcus</i> sp. W_1.2 and <i>Arthrobacter</i> sp. W_2.1 | - |
| <i>Planococcus</i> sp. W_1.2 | Overgrown by <i>Arthrobacter</i> sp. W_2.1 and <i>R. erythropolis</i> W_Sd5, inhibited of <i>R. erythropolis</i> W_Sd5 at contact point | - |
| <i>Arthrobacter</i> sp. W_2.1 | Highest growth rate, inhibited of W_Sd5 at contact point | Increased crystal accumulation near contact point |
| sLM | | |
| <i>Streptomyces</i> sp. sLM8 | | - |
| <i>Agromyces cerinus</i> sLM10 | | - |
| <i>Streptomyces</i> sp. sLM17 | Inhibited of <i>A. cerinus</i> sLM10 | - |
| <i>Bacillus</i> sp. sLM42 | Highest growth rate, overgrew all interaction strains | - |
| sMM | | |
| <i>Streptomyces</i> sp. sMM10 | Highest growth rate, overgrew <i>M. osloensis</i> sMM16 and <i>S. bauzanensis</i> sMM41 | - |
| <i>Moraxella osloensis</i> sMM16 | | Increased crystal accumulation at contact point to <i>Streptomyces</i> sp. sMM10 and <i>A. jejuensis</i> sMM51 |
| <i>Sphingopyxis bauzanensis</i> sMM41 | | +/- |
| <i>Agrococcus jejuensis</i> sMM51 | Inhibited by <i>M. osloensis</i> sMM16 | Increased crystal accumulation at contact point to <i>M. osloensis</i> sMM16 |

-, no crystals/no growth; +/-, low amount of crystals or low growth; blank cells, no visible effect

Gelöscht: compatriote

Gelöscht: in co-cultivation

Formatiert: Schriftart: Nicht Kursiv

Gelöscht: ion

Formatiert: Schriftart: Nicht Kursiv

Formatiert: Schriftart: Nicht Kursiv

Formatiert: Schriftart: Nicht Kursiv

Formatiert: Schriftart: Nicht Kursiv

Formatiert: Schriftart: Nicht Kursiv

Formatiert: Schriftart: Nicht Kursiv

Formatiert: Schriftart: Nicht Kursiv

Formatiert: Schriftart: Nicht Kursiv

Gelöscht: ion

Formatiert: Schriftart: Nicht Kursiv

Formatiert: Schriftart: Nicht Kursiv

Formatiert: Schriftart: Nicht Kursiv

Formatiert: Schriftart: Nicht Kursiv

Gelöscht: ion

Formatiert: Schriftart: Nicht Kursiv

Gelöscht: ion

Formatiert: Schriftart: Nicht Kursiv

Formatiert: Schriftart: Nicht Kursiv

Gelöscht: ion

Formatiert: Schriftart: Nicht Kursiv

Formatiert: Schriftart: Nicht Kursiv

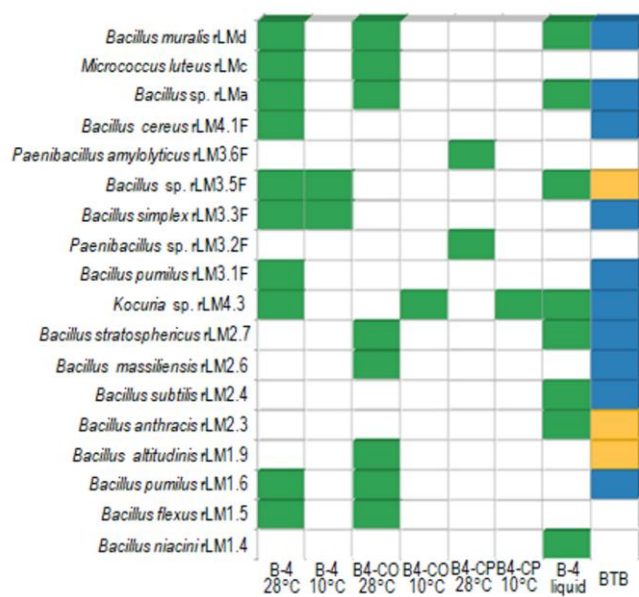
Formatiert: Schriftart: Nicht Kursiv

Gelöscht: ion

Table 3: Quantification of calcite precipitation by isolates from rock (r) and soil (s) of Lower (LM) and Middle Muschelkalk (MM). Similar cell counts were obtained. The dry weight of crystals was measured (see Material and Methods).

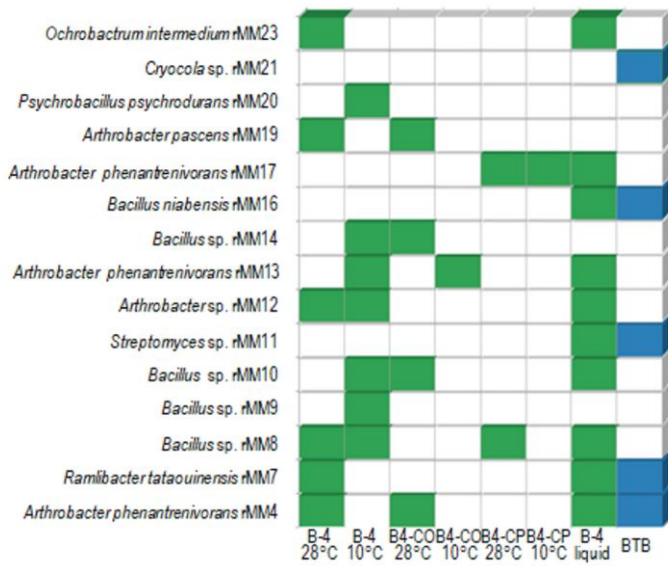
| Strain | Mean Coulter cell counter [cells/ml] | Dry weight [g/L] |
|-----------------------------------|--------------------------------------|------------------|
| <i>Bacillus muralis</i> rLMd | $3.97 \cdot 10^7$ | 0.064 |
| <i>Bacillus</i> sp. rMM9 | $5.77 \cdot 10^7$ | 0.104 |
| <i>Streptomyces</i> sp. sLM37 | $2.06 \cdot 10^7$ | 0.088 |
| <i>Agrococcus jejuensis</i> sMM51 | $8.65 \cdot 10^7$ | 0.096 |

Formatiert: Schriftart: Nicht Fett



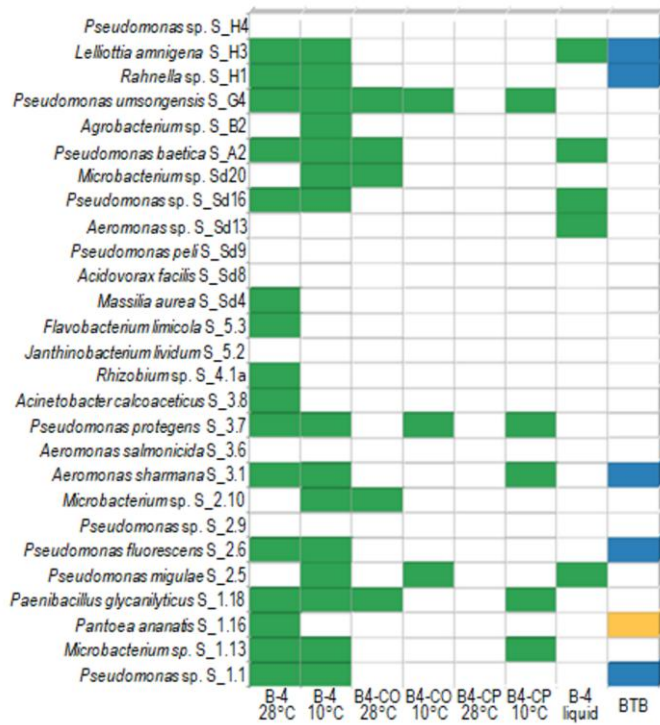
Formatiert: Schriftart: (Standard) Arial

5 **Figure 1: Mineral formation by all strains tested from rock of Lower Muschelkalk. The media used were B-4 with calcium acetate or B-4 with calcium carbonate (B4-CO) or calcium phosphate (B4-CP), all tested at 28°C or 10°C, and liquid B-4-medium at 28 °C. Changes in pH were visualized on indicator plates (BTB) with yellow for change to acidic and blue for change to alkaline pH (no growth indicated with blank cells on BTB medium; the pH reading was taken at the same time the mineral formation was scored). Crystal formation is indicated in green, no crystal formation in white. See text for more details.**



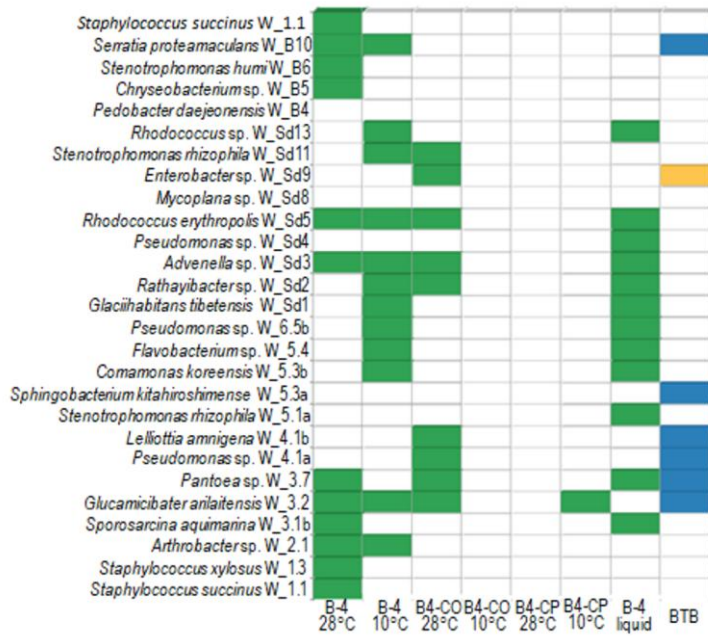
Formatiert: Schriftart: (Standard) Arial

Figure 2: Mineral formation by all strains tested from rock of Middle Muschelkalk. See legend of Fig. 1 for details.



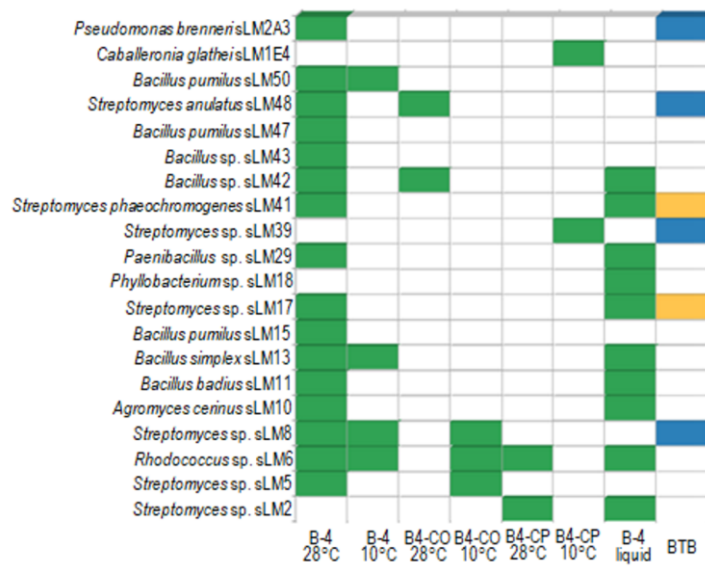
Formatiert: Schriftart: (Standard)
Arial, Fett

Figure 3: Mineral formation by all strains tested from groundwater in Stöben, Lower Muschelkalk. See legend of Fig. 1 for details.



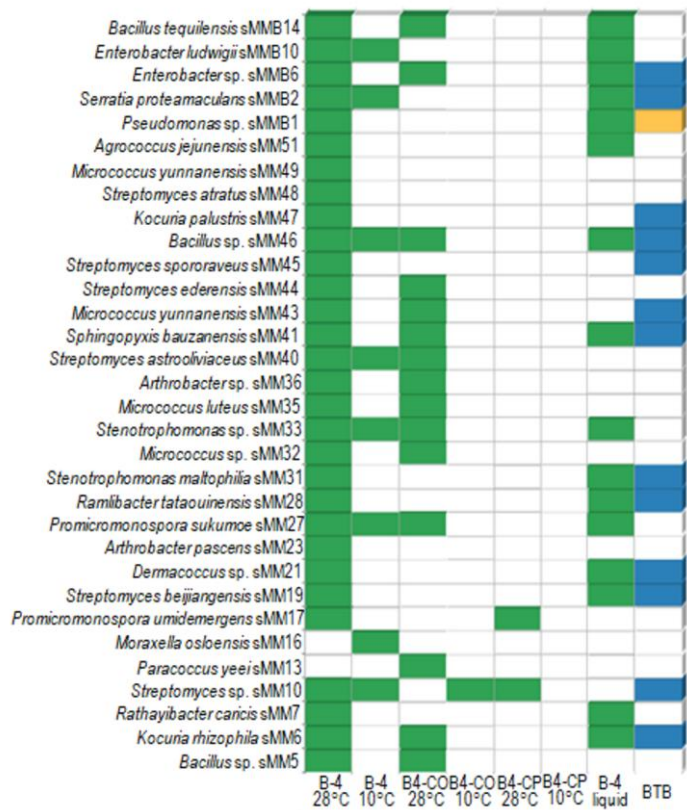
Formatiert: Schriftart: (Standard)
Arial, Fett

Figure 4: Mineral formation by all strains tested from groundwater in Wichmar, Middle Muschelkalk. See legend of Fig. 1 for details.



Formatiert: Schriftart: (Standard)
Arial, Fett

Figure 5: Mineral formation by all strains tested from soil on Lower Muschelkalk. See legend of Fig. 1 for details.



Formatiert: Schriftart: (Standard)
Arial, Fett

Figure 6: Mineral formation by all strains tested from soil on Middle Muschelkalk. See legend of Fig. 1 for details.

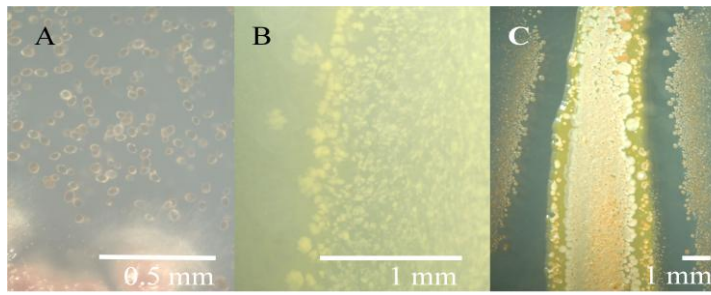


Figure 7: Crystal morphologies and distribution shown for selected strains. From Middle Muschelkalk soil *Moraxella osloensis* sMM16 formed brownish spherical crystals within the agar (A), from groundwater of Middle Muschelkalk at Wichmar *Glucanicibacter tibetensis* W_3.2 was recorded with flaky yellowish crystals on the culture (B), while from groundwater from Middle Muschelkalk at Wichmar *Arthrobacter* sp. W_2.1 showed a white crusts on the culture surface and reddish spherical crystals behind an inhibition zone (C).

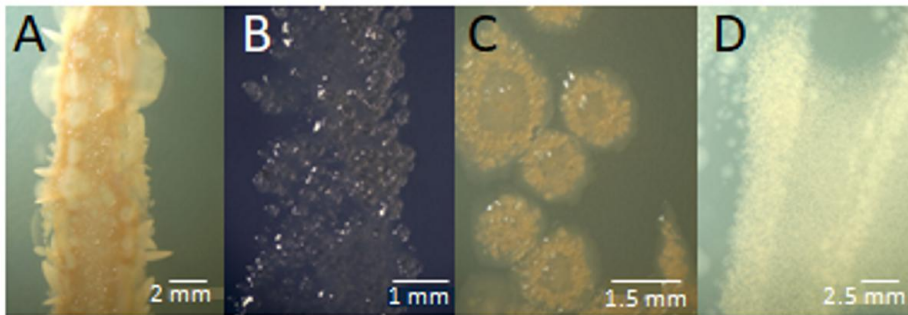


Figure 8: Mineral morphology is changed by growth temperature. *Pseudomonas* sp. S_1.1 at 28 °C (A) and 10 °C (B) shows not only induction of pigment formation, but also change from laminated shapes to transparent spheres. *Rahnella* sp. S_H1 at 28 °C forms rhombohedric to rosette like crystals at higher temperature (C), while small spheres are formed at 10 °C (D). Size bar, 1 mm.

Formatiert: Schriftart: (Standard)
Arial, Fett

Formatiert: Schriftart: Nicht Kursiv

Formatiert: Schriftart: Nicht Kursiv

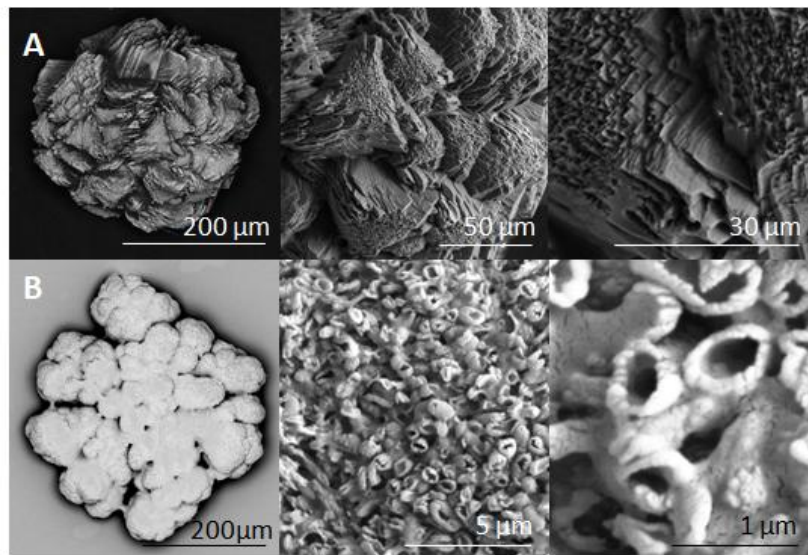


Figure 9: Scanning electron micrographs for crystal morphologies of minerals formed by *Lelliottia amnigena* S_H3 (panel A) and *Rhodococcus erythropolis* W_Sd5 (panel B), each illustrated at different magnifications. While the left images show the macromorphology, the detailed pictures give insight into surface and microcrystalline structures.